

## STAFF SUMMARY SHEET

	TO	ACTION	SIGNATURE (Surname), GRADE AND DATE		TO	ACTION	SIGNATURE (Surname), GRADE AND DATE
1	DFP	sig	Wohlwend, LT61, 24 OCT 13 <i>Wohlwend</i>	6			
2	DFER	approve	SOLTE, AD-22, 25 OCT <i>See (*) below</i>	7			
3	DFP	action		8			
4				9			
5				10			

SURNAME OF ACTION OFFICER AND GRADE

SYMBOL

PHONE

TYPIST'S

SUSPENSE DATE

Lane, Major

DFP

333-2460

mgm

SUBJECT

Clearance for Material for Public Release

USAF-DF-PA- 497

DATE

## SUMMARY

1. PURPOSE. To provide security and policy review on the document at Tab 1 prior to release to the public.

## 2. BACKGROUND.

Author: Jianqi Qin, Victor P. Pasko, Matthew G. McHarg and Hans C. Stenbaek-Nielsen

Title: Plasma Irregularities in the D-Region Ionosphere in Association with Sprite Streamer Initiation

Document type: Journal Article

Description: In this paper, the authors investigate irregularities in the D Region leading to streamer initiation in sprites.

Release Information: This document is being submitted for publication in Nature Geoscience

Previous Clearance information: None

Recommended Distribution Statement:

Distribution A, Approved for public release, distribution unlimited.

(\*) Add to bottom of 1st page

3. DISCUSSION. This research is funded by NSF.

4. VIEWS OF OTHERS. N/A

5. RECOMMENDATION. Sign coord block above indicating document is suitable for public release. Suitability is based solely on the document being unclassified, not jeopardizing DoD interests, and accurately portraying official policy.

// signed //

CORY T. LANE, Maj, USAF  
Director of Research  
Department of Physics

Tabs

1. Article

# Plasma Irregularities in the D-Region Ionosphere in Association with Sprite Streamer Initiation

Jianqi Qin<sup>1\*</sup>, Victor P. Pasko<sup>1</sup>, Matthew G. McHarg<sup>2</sup> and Hans C. Stenbaek-Nielsen<sup>3</sup>

<sup>1</sup>*Communications and Space Sciences Laboratory, Department of Electrical Engineering, Penn State University, University Park, Pennsylvania, USA*

<sup>2</sup>*Department of Physics, United States Air Force Academy, Colorado Spring, Colorado, USA*

<sup>3</sup>*Geophysical Institute, University of Alaska Fairbanks, Fairbanks, Alaska, USA*

Sprites are spectacular optical emissions in the mesosphere induced by transient lightning electric fields above thunderstorms. Although the streamer nature of sprites has been generally accepted, how these filamentary plasmas are initiated in the lower ionosphere remains a subject of active research and existing theories differ fundamentally from each other. Here we present a combination of observational and modeling results showing solid evidence of pre-existing plasma irregularities in association with sprite streamer initiation in the D-region ionosphere. The high-speed video observations show that prior to streamer initiation, spatial structures discernible in overall diffuse emissions of sprite halo descend rapidly with the halo, but slow down and stop to form the stationary glow in the vicinity of the streamer onset, from where streamers suddenly emerge. The modeling results reproduce the above-mentioned halo dynamics and demonstrate that the descending structures in the sprite halos are the optical manifestations of pre-existing plasma irregularities in the D-region ionosphere, which are necessary for streamer inception. An image processing algorithm is devel-

oped to reconstruct the plasma irregularities, showing that these plasma irregularities have a vertical dimension of a few kilometers and a horizontal dimension of a few hundred meters. The plasma irregularities might have been produced by thunderstorm or meteor effects on the D-region ionosphere.

From the Earth's surface to its ionosphere, the planet's atmosphere experiences an exponential decrease of its air density and an exponential increase of its electron density, leading to a transition region with unique properties in the altitude range of 60 to 90 km, known as the D region of the ionosphere, between the planet's lower atmosphere with dense air and its highly conducting ionosphere. For tropospheric thunderstorms, low electron density in this transition region enables the penetration of lightning electric fields, leading to many not yet well understood thunderstorm effects such as electron density fluctuations and depletions<sup>1,2</sup>, as well as occasionally the formation of spectacular sprite discharges<sup>3</sup>. Moreover, for meteor events, the D region is usually the lowest altitude region that meteoroids can reach due to significant friction caused by the rapid increase of air density, resulting in plasma irregularities observed as low-altitude meteor trail echoes in radar observations<sup>4</sup>.

Predicted in 1925 and first documented in 1989, sprite discharges originating from the D region ionosphere have been an active research area in the past two decades<sup>5,6</sup>. Early sprite theory emphasized the importance of thunderstorm activity since it was realized soon after the discovery that intense cloud-to-ground lightning discharges associated with large charge moment changes (i.e., charge times altitude from which it was removed) are necessary for their production<sup>7</sup>. Fol-

lowing that, the initiation of sprite streamers was interpreted in a modeling study as a result of the sharpening and collapse of the screening-ionization wave associated with the sprite halo when the lightning charge moment change was as large as  $1300 \text{ C km}^3$ . That theory encounters difficulties in explaining the temporal and spatial relations between sprite halo and sprite streamers<sup>9</sup>, and explaining them using experimentally observed (relatively small) charge moment changes with an empirical minimum of  $300 \text{ C km}^3$ . A different theory proposed recently overcomes these difficulties and indicates that the presence of strong plasma irregularities/inhomogeneities in the D region ionosphere is a necessary condition for the initiation of sprite streamers<sup>9,11</sup>, in agreement with recent experimental findings showing that a large charge moment change is a necessary but not sufficient condition for sprites<sup>12</sup>. However, up to date, no solid evidence of D-region plasma irregularities in association with sprite streamer initiation has been presented, and if these irregularities exist their characteristics and origin(s) remain unknown. In this study, we analyze high-speed video records of sprite-halo events and focus specifically on the halo dynamics prior to sprite streamer initiation. By comparing observational and numerical results, we demonstrate that the descending halo structures recorded in the high-speed video observations, from which sprite streamers are initiated, are optical manifestation of the pre-existing plasma irregularities. An image processing algorithm is then developed to reconstruct the characteristic shape and size of those plasma irregularities, showing that sprite halos can be effectively used to probe the plasma irregularities in the lower ionosphere. We further discuss origins of these plasma irregularities, suggesting possible relations between sprites and other thunderstorm effects or meteor events.

## 1 Origin of the Descending Halo Structures

In video observations, sprite-halo events exhibit a brief descending diffuse glow in the shape of a pancake with diameters up to  $\sim 80 \text{ km}$  near  $\sim 75 \text{ km}$  altitude, referred to as a sprite halo<sup>13</sup>, and develop into fine-structure filaments with diameters up to several hundred meters in the altitude range of  $\sim 40$  to  $\sim 90 \text{ km}$ , commonly referred to as sprite streamers<sup>14</sup>. Recent imaging of sprites at 16,000 fps indicates that prior to streamer initiation, spatial structures in halo emissions descend rapidly with the sprite halo, but slow down and stop to form the stationary glow in the vicinity of the streamer onset, from where streamers suddenly emerge and then accelerate exponentially<sup>3</sup>. The above-mentioned halo dynamics is illustrated in Figure 1.

The descending halo structures appear to be of essential importance for the initiation of sprite streamers. To understand the origin of those structures, it should be first emphasized that in the transient process of halo development on a typical time scale of  $\sim 1 \text{ ms}$ , free electrons in the lower ionosphere move only  $\sim 100 \text{ m}$  assuming an electron drift velocity of  $10^5 \text{ m/s}$ , which is negligible when compared to the descending distance of halo structures on the order of  $\sim 10 \text{ km}$ . In particular, in all halo events presented in this work, the electrons move upwards (i.e., in an opposite direction to the downward movement of the halos) due to the positive polarity of the causative lightning discharges. The observed descent of a sprite halo as an entire object is due to the increase of the large-scale lightning electric field at low altitudes and fast relaxation at high altitudes during the causative lightning discharge, leading to the lowering of the thin altitude region of large reduced electric field  $E/N$ , where  $N$  is the air density at the altitude of interest (i.e., the large-scale halo is

optical manifestation of the region of large reduced electric field in the lower ionosphere)<sup>9</sup>. Note that large reduced electric field leads to high rate of electron impact excitation of  $N_2$ , which is the main physical process accounting for the halo optical emissions. Thus the observed descent of halo structures, proceeding at the same pace as the large-scale halo emissions, is also due to the lowering of the thin altitude region of large reduced electric field. In other words, at each moment of time, the vertical dimension of the halo structures should be defined by the vertical structuring of the lightning reduced electric field. However, unlike its rapid spatial variation in the vertical direction, the lightning electric field varies slowly on a spatial scale of tens of kilometers in the horizontal direction, which cannot lead to the observed small-scale horizontal fluctuations in the halo emissions. Since the electron impact excitation rate is determined by the reduced electric field along with the local electron density, we propose that the physical parameter that determines the horizontal dimension of the halo structures should be the fluctuations in the ambient electron density (i.e., ambient plasma irregularities).

To demonstrate that the downward progression of the high reduced field region and the presence of plasma irregularities can account for the observed descending halo structures, we use a two-dimensional cylindrically symmetric plasma fluid model (see Methods section) to numerically reproduce the dynamics of the descending halo structures. Figure 2a shows the ambient electron density and the plasma irregularity assumed in the simulation domain. The plasma irregularity has a Gaussian distribution in the horizontal direction with a peak value of  $100 \text{ cm}^{-3}$  and a characteristic size of 2 km. In the vertical direction, the plasma irregularity is homogeneous and has a length of  $\sim 12 \text{ km}$ , comparable to the descending distance of halo structures shown in Figure 1. Panels b

and c in Figure 2 show the sprite halo emissions from the first positive band system of  $N_2$  at  $t=0.7 \text{ ms}$  and  $1.2 \text{ ms}$ , respectively. It is clear that at each moment of time, only a small portion of the plasma irregularity produces emissions that are brighter than those originating from other regions of the halo. The horizontal dimension of this portion is approximately equal to the assumed horizontal size of the plasma irregularity. Examination of the spatial variation of the lightning electric field at each moment of time shows that the bright portion of the plasma irregularity is located at the altitude region with the largest lightning reduced electric field, and the vertical dimension of the bright portion is determined by the vertical size of this altitude region. Figure 2d shows a 1.4-ms image time series of the modeled halo structure. We can see clearly that the bright portion of the plasma irregularity descends rapidly at the same pace as the remaining parts of halo emissions, but the descent slows down due to the decrease of lightning current, and at  $t=1.4 \text{ ms}$  sprite streamers start forming. The speed of the descent ( $7.6 \times 10^6 \text{ m/s}$ ) is comparable to that of the halo structure ( $6.4 \times 10^6 \text{ m/s}$ ) shown in Figure 1. We note that the streamer starts after the halo has faded due to a longer time scale ( $\geq 1 \text{ ms}$ ) required for streamer initiation at  $\sim 75 \text{ km}$  altitude when compared to the duration of the halo ( $\sim 1 \text{ ms}$  for typical lightning return strokes.) It also needs to be emphasized that although the model indicates the inception of a sprite streamer at  $t \approx 1.4 \text{ ms}$ , it cannot accurately simulate the dynamics of the sprite streamer at later moments of time due to the low spatial resolution ( $\sim 120 \text{ m}$ ) used in the large simulation domain. In the head of a streamer at  $\sim 70 \text{ km}$  altitude, the electron density could change one order of magnitude on a spatial scale of  $\sim 2 \text{ m}$ . This high electron density gradient requires sub-meter spatial resolution to simulate, which is beyond a practical resolution possible in a large simulation domain used. Nevertheless, as shown in Figure 2,

with a spatial resolution of  $\sim 120$  m, the model is fully capable of reproducing large-scale plasma dynamics that involves only low electron density gradients, such as the experimentally observed descending halo structures. Based on the above analysis and comparison, it can be concluded that the halo structures are originated from preexisting D-region plasma irregularities, and the descent of the halo structures is due to the lowering of the thin altitude region of large reduced electric field during the charge removal process of the causative lightning discharge.

## 2 Reconstruction of the Pre-existing Plasma Irregularities

Since at different moments of time during the lightning discharge, different portions of the plasma irregularity are effectively “illuminated” by the lightning quasi-static electric field, the descending halo structures recorded by high-speed video cameras can be used to reconstruct the shape and size of the plasma irregularities in the lower ionosphere. Figure 3a shows the plasma irregularity in the modeled sprite-halo event reconstructed using image series from  $t=0$  ms to 1.4 ms (see Figure 2d) and the image-processing algorithm described in the Methods section. Comparison between Figures 2a and 3a indicates that the plasma irregularity in the simulation domain can be well reconstructed. Figure 3b shows the D-region plasma irregularity reconstructed using high-speed video records of the sprite-halo event shown in Figure 1. We emphasize that the reconstructed image does not contain information about the vertical density variation, but only shows the shape and size of the plasma irregularity as manifested by optical emissions. Nevertheless, important information can be derived from it. First, sprite streamers can be easily identified because they are much brighter than the plasma irregularity and the halo. Second, the right streamer is initiated

from the lower tip of the plasma irregularity. Plasma irregularity responsible for the left streamer cannot be reconstructed because if presents it should be located above the available field of view of the camera. Third, the size of the plasma irregularity can be estimated using two different approaches. (1) Based on the altitude range of the entire image which is calculated assuming the sprite streamer was directly above the causative lightning discharge, the vertical and horizontal size of the plasma irregularity are, respectively,  $\sim 5$  km and  $\sim 1$  km. (2) Based on a 100 m typical diameter of sprite streamers documented in the existing literature<sup>15</sup>, the vertical and horizontal size of the plasma irregularity are, respectively,  $\sim 2.5$  km and  $\sim 0.5$  km. These two estimates are roughly consistent with each other. Note that it is possible that the plasma irregularity has a significantly longer vertical dimension than that revealed in Figure 3b, because the lightning electric field cannot penetrate into higher altitudes so that even if a significant portion exists at high altitudes, it cannot be “illuminated”.

To further demonstrate the characteristics of plasma irregularities in association with sprite streamer initiation, we analyze another sprite-halo event observed on 20 July 2012, in which multiple plasma irregularities can be identified in the halo. For this event, the halo emissions first appear at 06:27:17:157 860 UT ( $t=0$  ms). Figure 4a shows the halo emissions at  $t=1.04$  ms. Five bright halo structures are identifiable at this moment of time, and in the video record they all experience descending motion similar to that shown in Figure 1d. At  $t=1.28$  ms, a sprite streamer was already initiated from the leftmost halo structure. For all the other four halo structures,  $t=1.28$  ms is the moment just before the initiation of sprite streamers. Figure 4b shows the five plasma irregularities reconstructed using all video frames from  $t = 0$  to 1.28 ms. These plasma irregularities are

respectively responsible for the five descending halo structures (see Figure 4a) and the following five sprites (not all shown in Figure 4b). As an additional evidence, Figure 4c shows a halo event with no following sprite streamers. This halo event was observed on 14 July 2010 starting at 08:32:31.594 409 UT, and it has a typical pancake shape, which is defined by the spatial variation of the large-scale lightning electric field. In the reconstructed image shown in Figure 4d, no plasma irregularities and sprite streamers can be identified, which is an indirect evidence suggesting the importance of plasma irregularities for the initiation of sprite streamers.

A recently proposed theory suggests that the presence of strong plasma irregularities in the D-region ionosphere is a necessary condition for the initiation of sprite streamers<sup>9,11</sup>, and modeling results show that vertically elongated plasma columns are more favorable for streamer initiation when compared to spherical irregularities<sup>16,17</sup>. The above reconstructed images demonstrate for the first time solid evidence of kilometer-scale plasma irregularities in association with sprite streamer initiation in the D-region ionosphere. However, it is important to emphasize that not all the plasma irregularities in association with sprite streamer initiation can be observed as descending halo structures in video records of sprite events. Two reasons can lead to the absence of descending halo structures in sprite observations. First, the descending halo structures emphasized in the present work are due to a significant vertical dimension of the plasma irregularities leading to the effective illumination of a small portion of the plasma irregularities at each moment of time by the lightning electric field. In the case when the plasma irregularities are approximately spherical and have a compact size of tens to hundreds of meters, which are capable of initiating sprite streamers according to the previous modeling studies<sup>11,18</sup>, the plasma irregularities could only be recorded

as a local enhancement of the halo luminosity around the origin of sprite streamers. Second, the brightness of halos depends on the impulsiveness of the causative lightning return strokes<sup>18</sup>. In some sprite events, the halo and halo structures can remain sub-visual if the return stroke is not impulsive enough. We note that a relatively bright but not saturated large-scale halo is ideal for the reconstruction of the plasma irregularities. It has also been verified that in some cases when only the descending halo structures are visible, the reconstruction is also possible since halo structures are brighter than the other parts of the halo, that remain sub-visual.

### 3 Possible Origins of the Reconstructed Plasma Irregularities

According to previous modeling studies<sup>16,18</sup>, the electron density in plasma irregularities needs to be  $\sim 2$  to 5 orders of magnitude higher than the ambient electron density in order to initiate sprite streamers, depending on the onset altitude of the sprite streamers (at lower altitudes, the difference needs to be larger). It is reasonable to believe that such strong perturbations can not persist in a quiet lower ionosphere, and it is important to emphasize that the origin(s) of those plasma irregularities cannot be determined using the results presented in this work. The several possible origins are discussed below.

(1) Thunderstorm effects. Tropospheric thunderstorms are well-known to be able to disturb the lower ionosphere by convective atmospheric gravity waves and by lightning electric fields, leading to conductivity enhancement, electron density depletions, and D-layer reflection height splitting<sup>1,2,7,19</sup>. However, most of those are large spatial scale processes. The only known thunder-



storm effect that could produce the kilometer-scale plasma irregularities with a density enhancement of at least  $\sim 2$  orders of magnitude is sprites themselves. Previous modeling results suggest that the electron density enhancement in sprite bodies can typically last for approximately hundred seconds at  $\sim 75$  km altitude<sup>20</sup>. The remnant of a previous sprite body could indeed facilitate the initiation of sprites at tens of milliseconds later according to video observations<sup>21,22</sup>. To examine the possibility of previous sprites producing the plasma irregularities observed in Figures 1 and 4a, we have analyzed the images of sprites captured prior to those events on the same nights. We find that no previous sprites occurred at the same location as the one shown in Figure 1. For the event shown in Figure 4a, a sprite event occurred  $\sim 10$  minutes before, and the bright sprite columns captured by the same camera largely overlap with the sprites shown in Figure 4a. Unfortunately, images captured using another camera missed most parts of the two events so that the exact coincidence of the sprite locations cannot be verified using a triangulation technique. The  $\sim 10$  minutes time separation is much longer than the  $\sim 100$  s relaxation time of the electron density enhancement at  $\sim 75$  km altitude estimated in modeling of sprite chemistry<sup>20</sup>. On the other hand, recent coordinated radio and optical observations show that long recovery early VLF events, caused by long-lasting (a few hundred seconds to tens of minutes) D-region ionospheric conductivity modifications, occurred often coincidentally with bright sprites<sup>23</sup>. It has been suggested that the long-lasting conductivity modifications may have been produced by those concurrent sprites<sup>23</sup>. Although how the electron density enhancement in sprites could last so long is not clear, the plasma irregularities shown in Figure 4a might be related to the previous sprite event that occurred  $\sim 10$  minutes before.

(2) Meteor events. Considering the requirement of several orders of magnitude plasma den-

sity enhancement for streamer initiation, those plasma irregularities might have been produced by meteor events. Meteors had been suggested to be a possible factor for the initiation of sprite streamers in early sprite research, but soon the idea was discarded because using a visually observed meteor flux density of  $8 \times 10^{-7} \text{ km}^{-2} \text{ s}^{-1}$  it was estimated that for a sprite with a horizontal cross-sectional area of  $\sim 175 \text{ km}^2$  one would expect only  $\sim 10^{-4}$  sporadic meteors to intersect a sprite volume in a 1 s interval prior to the optical observation of the sprite<sup>24</sup>. However, radar observations show that visual and sub-visual meteors are continuously entering the Earth's upper atmosphere with a much larger flux density estimated to be  $\sim 10^{-5} \text{ km}^{-2} \text{ s}^{-1}$  globally<sup>25</sup>. Moreover, the entire volume of a large-scale halo, which covers a horizontal cross-sectional area of  $\pi R_{\text{halo}}^2 \sim 5000 \text{ km}^2$  assuming a radius  $R_{\text{halo}}$  of 40 km, should be used in the estimate because sprites could have lateral offsets as large as  $\sim 40$ -50 km with respect to the causative lightning discharge<sup>26</sup>. With these different values, it is estimated that on average 0.05 meteors could intersect a large-scale halo volume in a 1 s interval prior to sprite initiation. We note that the above estimate is rough as no observations are yet available quantifying the meteor flux density in a specific region above an active thunderstorm producing sprites. Nevertheless, this estimate suggests a higher probability (i.e., 5% using the methodology described above) of a positive correlation between sprite and meteor events than that shown in previous literature.

As a summary, a comparison of experimental and numerical results presented in this study demonstrates that the descending halo structures in sprite-halo events recorded by high-speed video cameras are the optical manifestation of pre-existing plasma irregularities in the D-region ionosphere. It is for the first time that robust evidence of plasma irregularities in association with

sprite streamer initiation is presented and the characteristic size of these plasma irregularities is quantified. Thunderstorm effects and meteor events are suggested to be two possible origins of those plasma irregularities. We note that future observations focusing on halo structures and modeling studies are necessary to understand the origin(s) of those D-region plasma irregularities in association with sprite initiation.

## Methods

**Plasma Fluid Model.** In our plasma fluid model<sup>18</sup>, the chemical reactions accounted for include the electron impact ionization of  $N_2$  and  $O_2$ , the electron dissociative attachment to  $O_2$ , and the electron detachment process  $O^- + N_2 \rightarrow e + N_2O$ . Note that although included, the effect of detachment in our simulations is negligible over a  $\sim 2$  ms time scale. Photoionization processes are included using the three-group  $SP_3$  model<sup>27</sup>. The motion of charged species is simulated by solving the drift-diffusion equations for electrons and ions coupled with the Poisson's equation<sup>18</sup>. The transport equations for charged species are solved using a flux-corrected transport technique that combines an eighth-order scheme for the high-order fluxes and a donor cell scheme for the low-order fluxes<sup>28</sup>. The simulation domain extends from ground up to 95 km, has a radius of 95 km, and is discretized using a grid with a spatial resolution of  $\sim 120$  m. It is assumed that perfectly conducting boundary conditions are satisfied on all boundaries of the simulation domain.

**Ambient Electron Density Profile.** The ambient electron density profile can be expressed as<sup>29</sup>:

$$n_e(h) = 1.43 \times 10^{13} e^{-0.15h'} e^{(\beta-0.15)(h-h')} \quad [m^{-3}] \quad (1)$$

where  $h'$  [km] and  $\beta$  [km<sup>-1</sup>] are given parameters describing reference altitude and sharpness, respectively. We assume that  $h'=85$  km and  $\beta=0.5$  km<sup>-1</sup>, which represent a typical nighttime electron density profile. The positive ion density  $n_{ion}$  is assumed to be equal to the electron density at high altitudes, where electron density is higher than  $10^8$  m<sup>-3</sup>, and is equal to  $10^8$  m<sup>-3</sup> at lower altitudes. Initial ambient negative ion density is then calculated based on charge neutrality.

**Lightning Current Waveform.** The waveform for lightning current moment is modeled using the following formulation<sup>30</sup>:

$$Ih_Q(t) = \frac{Qh_Q}{12t_0} \left( \frac{t}{t_0} \right) \exp \left[ - \left( \frac{t}{t_0} \right)^{1/2} \right] \quad (2)$$

where the lightning charge moment change  $Qh_Q$  is chosen to be 800 C km and  $t_0=25$   $\mu$ s that corresponds to a return stroke with a duration of  $\sim 1$  ms.

**The Image-Processing Algorithm.** To reconstruct the shape and size of the plasma irregularities, different image processing algorithms could be developed. Here we provide an illustration of a simple and effective algorithm developed as part of the present work. All frames from the beginning of the halo to streamer initiation are used in the reconstruction process. First, each frame is converted to a 8 bit gray scale image. Second, the intensity in each image is linearly normalized to equalize the peak intensity in different images. The purpose of this normalization is to make the brightness of the halo structures in different images that corresponds to different portions of the plasma irregularities comparable. The rationale of the normalization is explained as follows. The brightness of the halo structures in the original image time series could be significantly different from each other. This difference is mainly due to the temporal variation of the lightning reduced



electric field (see e.g., Figure 1 in the reference [11]), and may partially stem from vertical density variation in the plasma irregularities. In other words, difference in the brightness of the halo structures in different images does not necessarily indicate that the density in the body of a plasma irregularity varies significantly in the vertical dimension. As shown in Figure 2d, even if the plasma irregularity is assumed to be vertically homogeneous, temporal variation of the lightning electric field could still lead to significant difference in the brightness of the halo structure. Since our aim is to reconstruct the shape and size, rather than the density variation of the plasma irregularities, we remove the effect of lightning electric field variation by equalizing the peak intensity in the sprite images. This step is important as otherwise some parts of the plasma irregularities cannot always be reconstructed due to weak brightness when compared to other parts. In the final step, we compare the normalized images pixel by pixel retaining only the maximum intensity in each pixel and using these values to form the reconstructed image. Assuming that 10 normalized images are used in the reconstruction, and each has a total number of pixels  $M \times N$ . For each pixel denoted by  $(m, n)$ , there are 10 different intensity values  $I(m, n)$  from those 10 normalized images, among which the maximum one  $I_{\max}(m, n)$  is chosen to be the intensity in the pixel  $(m, n)$  of the reconstructed image. Using this algorithm, the halo structures captured in an image time series can be merged in a single image to reveal the shape and size of the plasma irregularities.

1. Lay, E. H. & Shao, X. M. High temporal and spatial-resolution detection of D-layer fluctuations by using time-domain lightning waveforms. *J. Geophys. Res.* **116**, A01317 (2011).
2. Shao, X.-M., Lay, E. H. & Jacobson, A. R. Reduction of electron density in the night-time

lower ionosphere in response to a thunderstorm. *Nat. Geosci.* **6**, 29–33 (2013).

3. Stenbaek-Nielsen, H. C., Kanmae, T., McHarg, M. G. & Haaland, R. High-Speed Observations of Sprite Streamers. *Surv. Geophys.* in press (2013).
4. Malhotra, A. & Mathews, J. D. Low-altitude meteor trail echoes. *Geophys. Res. Lett.* **36**, L21106 (2009).
5. Wilson, C. T. R. The electric field of a thundercloud and some of its effects. *Proc. Phys. Soc. London* **37**, 32D–37D (1925).
6. Franz, R. C., Nemzek, R. J. & Winckler, J. R. Television image of a large upward electric discharge above a thunderstorm system. *Science* **249**, 48–51 (1990).
7. Pasko, V. P., Inan, U. S., Bell, T. F. & Taranenko, Y. N. Sprites produced by quasi-electrostatic heating and ionization in the lower ionosphere. *J. Geophys. Res.* **102**, 4529–4561 (1997).
8. Luque, A. & Ebert, U. Emergence of sprite streamers from screening-ionization waves in the lower ionosphere. *Nat. Geosci.* **2**, 757–760 (2009).
9. Qin, J., Celestin, S. & Pasko, V. P. On the inception of streamers from sprite halo events produced by lightning discharges with positive and negative polarity. *J. Geophys. Res.* **116**, A06305 (2011).
10. Cummer, S. A. & Lyons, W. A. Implication of lightning charge moment changes for sprite initiation. *J. Geophys. Res.* **110**, A04304 (2005).

11. Qin, J., Celestin, S. & Pasko, V. P. Formation of single and double-headed streamers in sprite-halo events. *Geophys. Res. Lett.* **39**, L05810 (2012).
12. Lang, T. J. *et al.* Transient luminous events above two mesoscale convective systems: Charge moment change analysis. *J. Geophys. Res.* **116**, A10306 (2011).
13. Barrington-Leigh, C. P., Inan, U. S. & Stanley, M. Identification of sprites and elves with intensified video and broadband array photometry. *J. Geophys. Res.* **106**, 1741–1750 (2001).
14. Pasko, V. P., Inan, U. S. & Bell, T. F. Spatial structure of sprites. *Geophys. Res. Lett.* **25**, 2123–2126 (1998).
15. Kanmae, T., Stenbaek-Nielsen, H. C., McHarg, M. G. & Haaland, R. K. Diameter-speed relation of sprite streamers. *J. Phys. D-Appl. Phys.* **45**, 275203 (2012).
16. Liu, N., Kosar, B., Sadighi, S., Dwyer, J. R. & Rassoul, H. K. Formation of Streamer Discharges from an Isolated Ionization Column at Subbreakdown Conditions. *Phys. Rev. Lett.* **109**, 025002 (2012).
17. Kosar, B. C., Liu, N. & Rassoul, H. K. Luminosity and propagation characteristics of sprite streamers initiated from small ionospheric disturbances at sub-breakdown conditions. *J. Geophys. Res.* **117**, A08328 (2012).
18. Qin, J., Celestin, S. & Pasko, V. P. Dependence of positive and negative sprite morphology on lightning characteristics and upper atmospheric ambient conditions. *J. Geophys. Res.* **118**, 2623–2638 (2013).
19. Marshall, R. A. An improved model of the lightning electromagnetic field interaction with the D-region ionosphere. *J. Geophys. Res.* **117**, A03316 (2012).
20. Gordillo-Vazquez, F. J. Air plasma kinetics under the influence of sprites. *J. Phys. D: Appl. Phys.* **41**, 234016 (2008).
21. Stenbaek-Nielsen, H. C., Moudry, D. R., Wescott, E. M., Sentman, D. D. & Sabbas, F. T. S. Sprites and possible mesospheric effects. *Geophys. Res. Lett.* **27**, 3829–3832 (2000).
22. Sentman, D. D., Stenbaek-Nielsen, H. C., McHarg, M. G. & Morrill, J. S. Plasma chemistry of sprite streamers. *J. Geophys. Res.* **113**, D11112 (2008).
23. Haldoupis, C., Cohen, M., Cotts, B., Arnone, E. & Inan, U. Long-lasting D-region ionospheric modifications, caused by intense lightning in association with elve and sprite pairs. *Geophys. Res. Lett.* **39**, L16801 (2012).
24. Suszcynsky, D. M. *et al.* Video and photometric observations of a sprite in coincidence with a meteor-triggered jet event. *J. Geophys. Res.* **104**, 31361–31368 (1999).
25. Verbeeck, C. Meteoroid flux densities from radio observations: the latest developments (2009). International Meteor Conference, The International Meteor Organization, Porec, Croatia, 24–27 Sept.
26. Wescott, E. M. *et al.* Triangulation of sprites, associated halos and their possible relation to causative lightning and micrometeors. *J. Geophys. Res.* **106**, 10467–10478 (2001).

27. Bourdon, A. *et al.* Efficient models for photoionization produced by non-thermal gas discharges in air based on radiative transfer and the Helmholtz equations. *Plasma Sources Sci. Technol.* **16**, 656–678 (2007).
28. Zalesak, S. T. Fully multidimensional flux-corrected transport algorithms for fluids. *J. Comput. Phys.* **31**, 335–362 (1979).
29. Wait, J. R. & Spies, K. P. *Characteristics of the Earth-ionosphere waveguide for VLF radio waves*, Tech note 300 (National Bureau of Standards, Boulder, Colorado, 1964).
30. Cho, M. & Rycroft, M. J. Computer simulation of the electric field structure and optical emission from cloud-top to the ionosphere. *J. Atmos. Solar Terr. Phys.* **60**, 871–888 (1998).

**Acknowledgements** This research was supported by the Defense Advanced Research Projects Agency and by the Physical and Dynamic Meteorology and the Aeronomy Programs of National Science Foundation. We thank J. Mathews for useful discussion about possible relation between sprites and meteors.

**Author contributions** J.Q. drafted the manuscript, developed the plasma fluid model, interpreted simulation results and compared them with the observations. V.P.P supervised the project. M.G.M and H.C.S. operated the sprite observations, derived the altitude range of the images. All authors contributed to the discussion of the results and the preparation of the manuscript.

**Competing financial interests** The authors declare no competing financial interests.

**Correspondence** Correspondence and requests for materials should be addressed to Jianqi Qin (jianqi.qin@psu.edu).

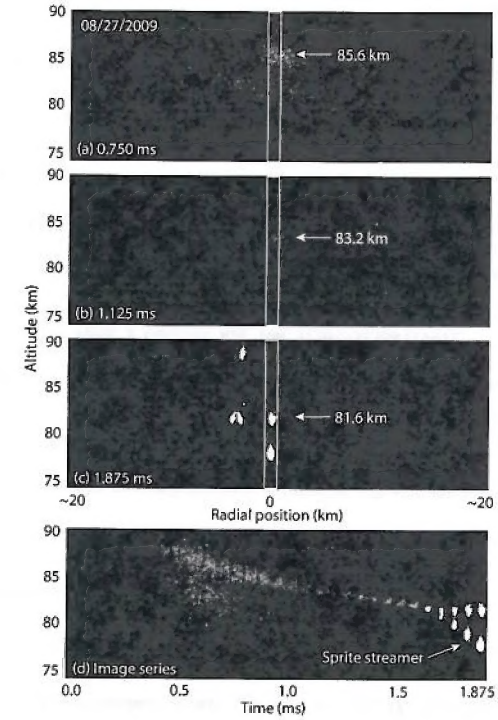


**Figure 1: A sprite-halo event observed on August 27, 2009.** The event starts at 09:15:23 085 570 UT ( $t=0$  ms). The frame rate of the camera is 16,000 fps. Images (a, b) respectively show the halo emissions at  $t=0.750$  ms and 1.125 ms, between which the halo structure descends with an average downward speed of  $6.4 \times 10^6$  m/s. Image (c) shows the sprite streamer initiated from the descending spatial structure. Panel (d) shows a 1.875-ms image time series of the halo structure and streamer development.

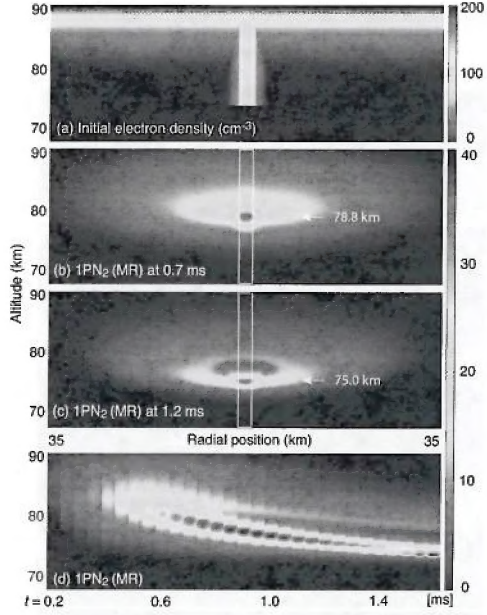


Figure 2: Descending halo structure observed in a halo modeling. (a) Ambient electron density and the plasma irregularity in the simulation domain. (b, c) Halo emissions from the first positive band system of  $\text{N}_2$  at  $t=0.7$  ms and 1.2 ms, respectively, between which the bright portion descends downward at average speed of  $7.6 \times 10^6$  m/s. (d) A 1.4-ms image time series of the modeled halo structure.

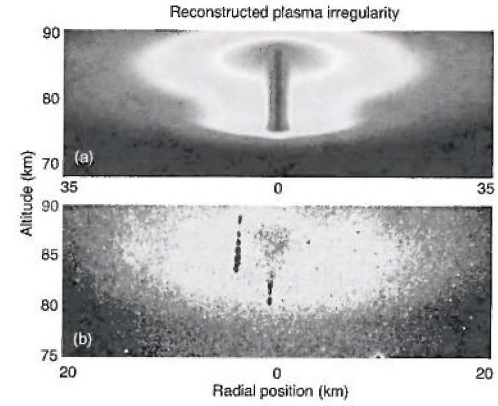


Figure 3: Reconstructed plasma irregularities. (a) The plasma irregularity reconstructed using image series from  $t=0$  ms to 1.4 ms corresponding to the model event shown in Figure 2. (b) The D-region plasma irregularity reconstructed using image series of the sprite halo event shown in Figure 1.



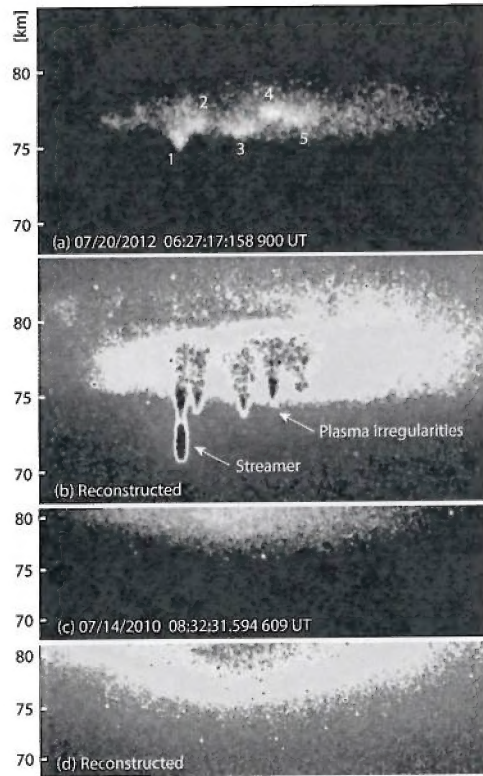


Figure 4: Halo events with and without plasma irregularities. (a, b) A frame of the sprite halo event observed on 20 July 2012 and the reconstructed image showing five plasma irregularities. (c, d) A frame of the halo event observed on 14 July 2010 and the reconstructed image that shows only large-scale halo emissions.